Adsorption of carbonate and bicarbonate salts at the air–brine interface

ARTICLE *in* INTERNATIONAL JOURNAL OF MINERAL PROCESSING · DECEMBER 2006

Impact Factor: 1.31 · DOI: 10.1016/j.minpro.2006.07.016 · Source: OAI

4 AUTHORS, INCLUDING:

Orhan Ozdemir
Istanbul University
53 PUBLICATIONS **683** CITATIONS
SEE PROFILE

Stoyan I Karakashev
Sofia University "St. Kliment Ohridski"
73 PUBLICATIONS **593** CITATIONS
SEE PROFILE

Jan D Miller
University of Utah
557 PUBLICATIONS **6,899** CITATIONS
SEE PROFILE

Available online at www.sciencedirect.com
ScienceDirect
Int. J. Miner. Process. 81 (2006) 149–158
INTERNATIONAL JOURNAL OF MINERAL PROCESSING
www.elsevier.com/locate/ijminpro

Adsorption of carbonate and bicarbonate salts at the air–brine interface

Orhan Ozdemir [a], Stoyan I. Karakashev [b], Anh V. Nguyen [b], Jan D. Miller [a,*]

[a] Department of Metallurgical Engineering, University of Utah, 135 South 1460 East 412 WBB, Salt Lake City, Utah 84112, USA
[b] Discipline of Chemical Engineering, School of Engineering, The University of Newcastle, University Drive, Callaghan, NSW 2308, Australia

Received 31 May 2006; received in revised form 20 July 2006; accepted 21 July 2006
Available online 26 September 2006

Abstract

Previous research has shown that the flotation of soluble salt is determined by interfacial water structure, thermal stability, and viscosity. These salts include alkali halide and alkali oxyanion salts. Of particular interest are the carbonate salts such as those associated with the great trona deposit of the Green River basin in Wyoming. In this study, we investigated the adsorption of carbonate and bicarbonate salts at the air–brine interface and correlated the adsorption behavior with water structure. Specifically, the equilibrium and dynamic surface tensions of sodium carbonate and sodium bicarbonate salts have been measured as a function of the salt concentration up to saturation and compared with the model prediction using the Gibbs–Langmuir adsorption theory. The results show that the negative adsorption of sodium carbonate leads to a significant increase in surface tension of the brine solution. For sodium bicarbonate, both the negative adsorption and the increase in surface tension are significantly lower when compared with the sodium carbonate case. The negative adsorption is correlated with the water structure making/breaking character of carbonate and bicarbonate solutions. In particular, sodium ions are significantly more hydrated than carbonate and bicarbonate ions, and, therefore, tend to be excluded from the air–brine interface. On the other hand, carbonate and bicarbonate ions are accommodated at the air–brine interface. In any event, the balance between sodium exclusion and carbonate/bicarbonate accommodation results in an increase in the surface tension of these solutions with an increase in salt concentration.

Keywords: Trona; Sodium carbonate; Sodium bicarbonate; Adsorption; Surface tension; Water structure maker and breaker

1. Introduction

Trona ($Na_2CO_3 \cdot NaHCO_3 \cdot 2H_2O$) is a complex salt of sodium carbonate (Na_2CO_3) and sodium bicarbonate ($NaHCO_3$). In the United States, trona is the major source of soda ash which is an essential raw material for glass, chemicals, detergents, and other important industries (Garrett, 1991). Recently, a special flotation procedure was proposed to separate the gangue minerals from trona ore and make a trona concentrate of 99% purity (Wang et al., 2002). Flotation of trona must be carried out in its saturated solution due to the high solubility of the trona (~1 mol/L). And this high salt concentration will make significant changes in the interfacial water structure which effects collector adsorption at the surface of soluble salt mineral particles and at the air–brine interface. In concentrated brines, water molecules strongly adsorbed at salt surfaces serve as a barrier that inhibits not only collector adsorption but also air bubble attachment at the salt

* Corresponding author.
E-mail address: jdmiller@mines.utah.edu (J.D. Miller).

0301-7516/$ - see front matter © 2006 Published by Elsevier B.V.
doi:10.1016/j.minpro.2006.07.016

surface (Hancer et al., 1997, 2001; Hancer and Miller, 1999).

Our fundamental studies with carbonate and bicarbonate salts indicate that $NaHCO_3$ can be floated with both 12C anionic and cationic collectors, whereas Na_2CO_3 does not float with either collector (Ozcan and Miller, 2002). Previous studies showed that the flotation of soluble salts depends on their structure breaking or structure making properties (Hancer et al., 2001). According to this study, some salts which increase the viscosity of the water are called structure makers (higher viscosity brine/hydrated surface), while some salts which do not change the viscosity of water significantly are called structure breaker salts (lower viscosity brine/less hydrated surface). A study of water structure making/breaking properties of Na_2CO_3 and $NaHCO_3$ using FTIR transmission spectroscopy showed that Na_2CO_3 has a very strong water structure making effect, while $NaHCO_3$ shows a weak water structure making effect (Nickolov et al., 2003). In this case, it is concluded that the structure breaking sodium bicarbonate ($NaHCO_3$) salt can be floated with both 12C anionic and cationic collectors, but the structure making sodium carbonate (Na_2CO_3) does not float due to the inability of the collector to break the organized water structure and adsorb at the surface of the carbonate particles. Even though the conditions have been fairly well established for the flotation of $NaHCO_3$, fundamental details of the interfacial phenomena require further study. Water structure as influenced by salt concentration is more complicated than simply considering a salt as a structure maker or structure breaker (Du et al., submitted for publication; Koneshan et al., 1998). Nevertheless such an approach is a convenient first approximation.

The aim of this paper is to investigate the adsorption of sodium carbonate and bicarbonate at the air–brine interface to determine if such adsorption is related to the water structure making/breaking character of the salts. The adsorption was experimentally determined in terms of dynamic and equilibrium surface tension measurements and theoretically examined applying the Gibbs–Langmuir adsorption theory.

2. Experimental

2.1. Materials

Sodium carbonate and bicarbonate salts (EMD Chemicals and Mallinckrodt) used in this study were of reagent grade. Deionized water obtained with a Milli-Q plus Millipore Ultra Pure Water system (Millipore Ltd., Molshem, France) was used in all the experiments. The quality of the deionized water was quantified using the conductivity and bubble persistence tests. The conductivity of the deionized water was about 0.686 S/m. The bubbles persisted on the surface of the water for less than 0.15 s, indicating no significant surface contamination of the deionized water. Surface tension of the deionized water was about 72.7 mN/m. All salt solutions were freshly prepared and used.

The needle and syringe used in measuring surface tension were cleaned using 6% (by volume) of Deconex 15E solution (Borer, Switzerland) and rinsed with distilled water several times. Before and between measurements, the surface tension of the deionized water was measured and compared with the available data to ensure that no contamination was present in the system. All glassware and the other components used in the experiments were soaked for several hours in the Deconex 15E solution, rinsed in the Milli-Q water, and dried in a cabinet to protect them from dust. The experiments were carried out at room temperature (~23 °C).

2.2. Apparatus

Adsorption was experimentally determined by measuring the dynamic surface tension versus concentration using pendant bubble tensiometry with a fully computer-controlled apparatus (System OCA 20, DataPhysics, Germany). The schematic of the experimental setup is shown in Fig. 1. The bubbles used in the pendant bubble tensiometry were enclosed by the solutions and, hence, the effect of evaporation on surface tension measurements was significantly small.

The setup was used to create a pendant bubble, the bubble silhouette was digitized, and the image data processed. The image forming and recording system consisted of a constant-intensity light source with a heat filter, a lens system for producing a collimated beam, an optically transparent cell enclosed in a thermostatically controlled chamber, and a CCD video camera fitted with long-working distance objective lenses. The camera was connected to a digitizer and a computer for image and data storage. The drop-forming system is connected to the computer-control system via a PC card, and a gas-tight micro-syringe fitted with a motorized syringe pump is driven by the computer.

2.3. Experimental method and procedure

Measurements of the dynamic surface tension of bubbles in salt solutions were undertaken as follows: an air bubble was formed at the end of the needle with the outer diameter of 1.622 mm by the use of the micro-syringe and the syringe pump as shown in Fig. 1. The

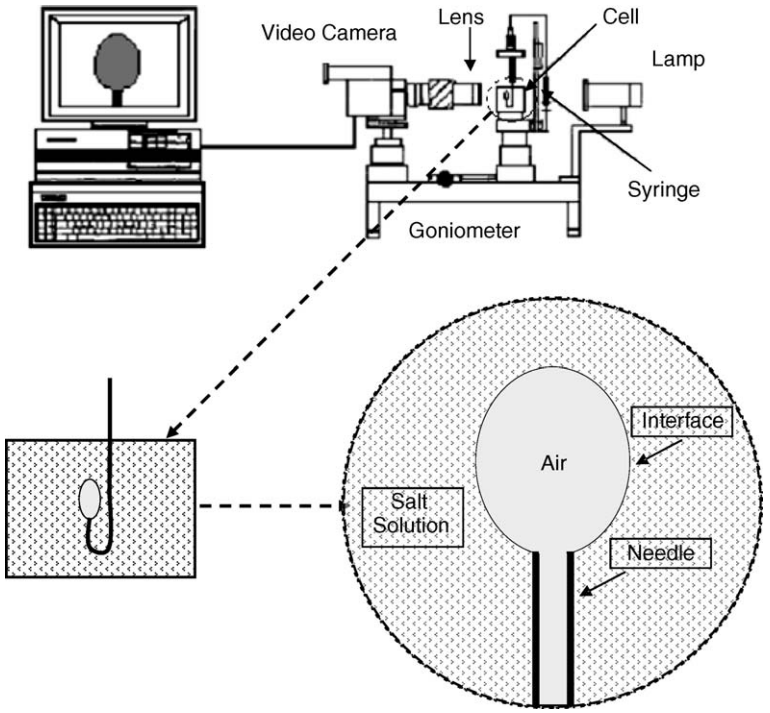

Fig. 1. A schematic of the pendant bubble tensiometer and the video image digitization equipment used to determine the dynamic and equilibrium surface tension of salt solutions.

bubble volume was approximately 20 μL. The time of formation of the bubble was about 1 s. The system was calibrated using the outer diameter of the needle. The bubble was placed in the path of a collimated light beam. The light beam cast a silhouette of the bubble shape onto the CCD camera. The camera was set to strobe, thereby obtaining the bubble shape as a function of time. Images of the bubbles were taken at the frequency of 50 Hz. The bubble shapes were digitized and analyzed offline.

The shape of a bubble is governed by the Young–Laplace equation, which relates the pressure drop across a curved interface by

$$\sigma\left(\frac{1}{R_1}+\frac{1}{R_2}\right)=\Delta P \tag{1}$$

where R_1 and R_2 are the two principal radii of the gas–liquid interface, and ΔP is the pressure difference across the interface. Since the pendant bubbles have rotational symmetry, the two principal radii can be described in terms of the profile coordinates of bubble images (Hartland and Hartley, 1976). The pressure difference ΔP in Eq. (1) is balanced by the local hydrostatic pressure on the interface, which is a function of the bubble profile coordinates.

The Young–Laplace equation was described as a second order differential equation in terms of the bubble profile coordinates and was solved numerically. The digitized bubble profiles were fitted numerically with the solution of the Young–Laplace equation to obtain the surface tension value. The numerical solution and fitting were carried out for each bubble image and the surface tension corresponding to each bubble image at given time was found, giving the dependence of surface tension on time (bubble age). With the salts studied, the surface tension at equilibrium was established very quickly (when the surface tension versus time reached a constant level). The best fits with the Young–Laplace equation and the highest accuracy of the measured surface tension were found with the largest bubbles having maximum deviation from the spherical shape of the bubbles. Bubble size was controlled by the time given for bubble formation.

3. Results and discussion

3.1. Surface tension of Na_2CO_3 and $NaHCO_3$ solutions at room temperature

The presence of salts in solution changes the properties of both the air–water and solid–water interfaces and these

electrolytes determine the interaction between particles and bubbles during flotation. For this reason it is important to understand how the electrolytes behave at the interfaces. The surface tension versus time (bubble age) is shown in Figs. 2 and 3 for the Na_2CO_3 and $NaHCO_3$ solutions, respectively. As can be seen from the figures, the adsorption of the salts onto the gas–liquid interface is extremely fast (within a second) and the surface tension of salt solutions does not significantly change with time.

The surface tensions at equilibrium for Na_2CO_3 and $NaHCO_3$ solutions were obtained by averaging the data shown in Figs. 2 and 3, and the results are summarized in Tables 1 and 2, respectively. The data shown in the tables were obtained with 5 different bubbles for a given concentration of salt. It is seen that the reproducibility of the measurements is excellent. The surface tensions of the salt solutions increase with increasing salt concentration up to the saturation concentrations, which are about 1.1 and 2.3 mol/L for $NaHCO_3$ and Na_2CO_3, respectively. The equilibrium surface tensions are plotted against the salt concentration in Fig. 4. The dependence of the equilibrium surface tension on concentration of Na_2CO_3 is strong and highly nonlinear. The surface tension for $NaHCO_3$ solutions shows a significantly weaker dependence on concentration than is the case for Na_2CO_3 solutions.

3.2. Modeling of adsorption and surface tension of Na_2CO_3 and $NaHCO_3$ brine solutions

An increase in surface tension in the presence of electrolytes has been explained by negative adsorption of ions at gas–water interface, however, some salts such as HCl, HNO_3, etc., decrease the surface tension of the water so that they positively adsorb at the air–water interface (Weissenborn and Pugh, 1996).

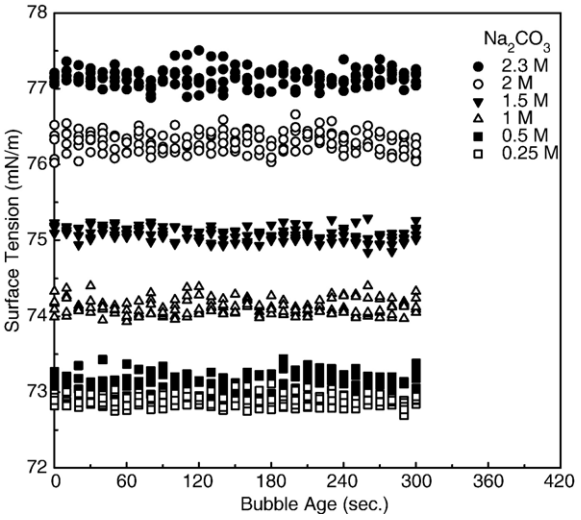

Fig. 2. Surface tension of Na_2CO_3 solutions versus time as described by bubble age.

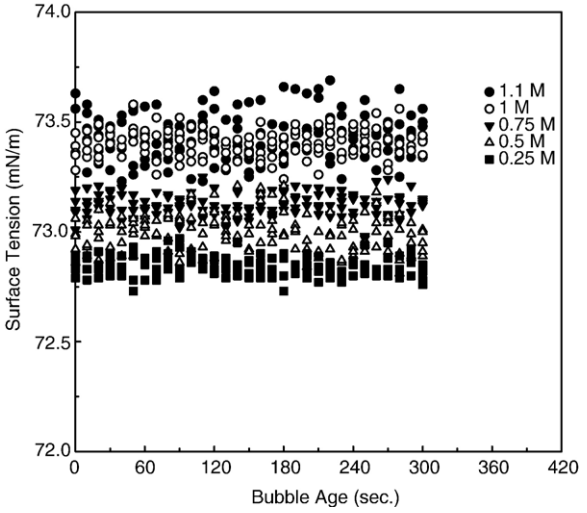

Fig. 3. Surface tension of $NaHCO_3$ solutions versus time as described by bubble age.

The experimentally observed increase in surface tension is evidently due to the "negative adsorption"[1] of sodium carbonate and bicarbonate salts at the air–brine interface. To describe the effect of negative adsorption on surface tension we adapt the traditional approach for modeling surfactant adsorption. The starting point is the Langmuir adsorption equation, which can be described for cation, M, and anion, X, dissociated from a single salt, MX, as

$$K_M a_M = \frac{\Gamma_M}{(-\Gamma_{M_\infty})-\Gamma_M} \tag{2}$$

$$K_X a_X = \frac{\Gamma_X}{\Gamma_{X_\infty}-\Gamma_X} \tag{3}$$

where Γ's with the subscripts M and M_∞ (or X and X_∞) describe the Gibbs surface excess for cations (or anions) and the maximum of the surface excess (in the absolute value), respectively; a with an appropriate subscript describes the ion activity in the solution at a given salt concentration and temperature; K with an appropriate subscript describes the equilibrium adsorption constant. Eqs. (2) and (3) can be obtained from the balance between the adsorption and desorption rates at equilibrium. The

[1] The term "negative adsorption" usually means the concentration of the solutes at the surface region is lower than in the bulk solution.

minus sign before Γ_{M_∞} on the right-hand side of Eq. (2) is obtained by considering the negative adsorption ($\Gamma_{M_\infty}<0$) of the cation (sodium ions) which are expelled by the interface. The negative adsorption of anions was also considered but the model did not agree with the experimental data for the measured surface tension. Therefore, it seems that adsorption of anions is positive and similar to the adsorption of surfactants. The Gibbs surface excess is an algebraic variable determined by the difference between the species concentrations in the bulk solution and at the interface, defined relative to the Gibbs dividing surface. Consequently, the Gibbs surface excess can be negative (Adamson and Gast, 1997).

The link between the Gibbs surface excess and surface tension now is established based on the Gibbs adsorption equation (Adamson and Gast, 1997):

$$d\sigma = RT[-\nu_X\Gamma_X d(\ln a_X)-\nu_M\Gamma_M d(\ln a_M)] \quad (4)$$

where ν_M and ν_X are the stoichiometric coefficients of the salt. Inserting Eqs. (2) and (3) into the Gibbs equation, and integrating gives

$$\sigma = \sigma_0 + \nu_X\Gamma_{X_\infty}RT\ln\left(1-\frac{\Gamma_X}{\Gamma_{X_\infty}}\right) - \nu_M\Gamma_{M_\infty}RT\ln\left(1+\frac{\Gamma_M}{\Gamma_{M_\infty}}\right) \quad (5)$$

where σ and σ_0 describe the surface tensions of the salt solution and pure solvent (water), respectively, R is the universal gas constant, and T is the absolute temperature. The second term on the right-hand side of Eq. (5) describes the effect of anion adsorption which tends to decrease the surface tension. Eq. (5) with the first two terms on the right-hand side is similar to the empirical Szyszkowski equation (Leja, 1982) which was developed for surfactants (Von Szyszkowski, 1908). The third term on the right-hand side of Eq. (5) describes the increase in the surface tension due to the negative adsorption of the cations.

Table 1
Average equilibrium tension of Na_2CO_3 solutions versus concentration at 23 °C

Concentration (mol/L)	Surface tension (mN/m)	Standard deviation (mN/m)
0	72.72	0.03
0.25	72.88	0.02
0.5	73.14	0.02
1.0	74.12	0.04
1.5	75.08	0.02
2.0	76.29	0.04
2.3 (saturation)	77.15	0.04

Table 2
Average equilibrium tension of $NaHCO_3$ solutions versus concentration at 23 °C

Concentration (mol/L)	Surface tension (mN/m)	Standard deviation (mN/m)
0	72.72	0.03
0.25	72.84	0.01
0.50	73.00	0.01
0.75	73.12	0.01
1.0	73.40	0.03
1.1 (saturation)	73.44	0.03

Therefore, Eq. (5) is significant for salt adsorption, which can have one ion type adsorbed at the interface and the other ions (with negative adsorption) being excluded from the interface. The Gibbs surface excess as a function of activity can be obtained by solving Eqs. (2) and (3), giving

$$\Gamma_M = \Gamma_{M_\infty}\frac{-K_M a_M}{1+K_M a_M} \quad (6)$$

$$\Gamma_X = \Gamma_{X_\infty}\frac{K_X a_X}{1+K_X a_X} \quad (7)$$

The activity used in Eqs. (2)–(5) for the brine solutions can be related to concentration using the Pitzer theory (Pitzer, 1973; Pitzer and Mayorga, 1973, 1974; Pitzer and Kim, 1974), which gives $a=\gamma m$, where γ is the activity coefficient and m is the molality concentration (mol per kg of solvent) of the salt. For the activity coefficient of ions dissociated from single salts described as MX, the Pitzer theory gives

$$\ln\gamma_M = -z_M^2 A\left[\frac{\sqrt{I}}{1+b\sqrt{I}}+\frac{2}{b}\ln\left(1+b\sqrt{I}\right)\right] + m_X\left(2B_{MX}+\frac{m_M C^{\varphi}_{MX}}{|z_X/z_M|^{1/2}}\right) + m_M m_X\left(\frac{z_M^2 B'_{MX}+z_M C^{\varphi}_{MX}}{|z_M z_X|^{1/2}}\right) \quad (8)$$

$$\ln\gamma_X = -z_X^2 A\left[\frac{\sqrt{I}}{1+b\sqrt{I}}+\frac{2}{b}\ln\left(1+b\sqrt{I}\right)\right] + m_M\left(2B_{MX}+\frac{m_M C^{\varphi}_{MX}}{|z_X/z_M|^{1/2}}\right) + m_M m_X\left(\frac{z_X^2 B'_{MX}+z_X C^{\varphi}_{MX}}{|z_M z_X|^{1/2}}\right) \quad (9)$$

where z_M and z_X are charge of cation M and anion X, respectively, $b=1.2$ is an empirical parameter. The ionic strength is defined as $I=(m_M z_M^2+m_X z_X^2)/2$, where m_M

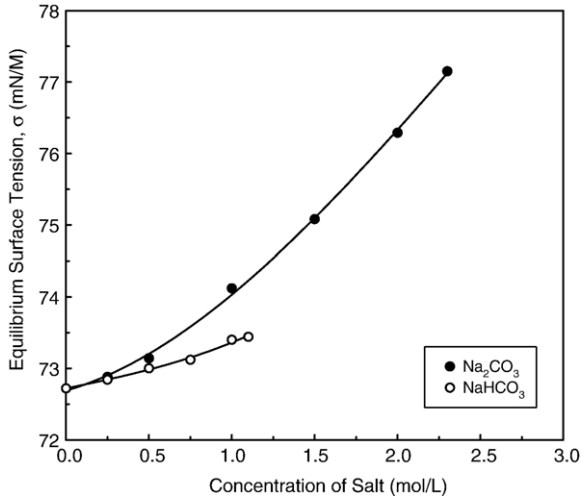

Fig. 4. Average equilibrium surface tension of Na_2CO_3 and $NaHCO_3$ brine solutions versus concentration up to the point of saturation.

and m_X are the molality concentration of the cations and anions, respectively. The Debye-Hückel coefficient, A, in Eqs. (8) and (9) is defined as; $A=(2\pi N_A d_w/1000)^{1/2}(4\pi\varepsilon_w\varepsilon_0 k_B T/e^2)^{-3/2}/3$, where N_A is the Avogadro number, e is the charge of a proton, k_B is the Boltzmann constant, ε_0 is the permittivity of vacuum, and d_w and ε_w are the density and relative dielectric constant of water, respectively. The value $A=0.392$ is usually used in calculating Eqs. (8) and (9) at 25°C. C^{ϕ}_{MX} in these equations is the Pitzer parameter related to the third virial coefficients.

In Eq. (8), B_{MX} and B'_{MX} describe the interaction parameters for the oppositely charged ions which are defined as explicit functions of the ionic strength by

$$B_{MX} = \beta_0 + \beta_1 f\left(\alpha_1 I^{1/2}\right) + \beta_2 f\left(\alpha_2 I^{1/2}\right) \quad (10)$$

$$B'_{MX} I = \beta_1 f'\left(\alpha_1 I^{1/2}\right) + \beta_2 f'\left(\alpha_2 I^{1/2}\right) \quad (11)$$

where β_i for $i=0$, 1, and 2 are the Pitzer coefficients determined by the second virial coefficients, and functions f and f' are defined as $f(x)=2[1-(1+x)\exp(-x)]/x^2$ and $f'(x)=2[1-(1+x+0.5x^2)\exp(-x)]/x^2$, respectively. For univalent electrolytes, only the first two terms of Eq. (10) and only the first term of Eq. (11) are considered where $\alpha_1=2$. For higher valence type electrolytes, such as 2–2 electrolytes, the full equations are used and $\alpha_1=1.4$ and $\alpha_2=12$.

Table 3
The Pitzer coefficients for Na_2CO_3 and $NaHCO_3$ (Kim and Frederick, 1988)

Salt	β_0	β_1	C^{ϕ}_{MX}
Na_2CO_3	0.05306	1.29262	0.00094
$NaHCO_3$	0.028	0.044	0

The Pitzer coefficients for Na_2CO_3 and $NaHCO_3$ are described in Table 3. The conversion of the molar, C, to molality, m, concentrations and verse versa can be carried out using experimental data for solution density.

The dependence of the activity for the sodium, carbonate and bicarbonate ions on the salt concentration for Na_2CO_3 and $NaHCO_3$ was calculated using the activity coefficient given by Eq. (8) and is shown in Fig. 5. As can be observed from this figure, the dependence of the activities of the ions on the concentration is not linear. The activity of carbonate ions is significantly smaller than the activity of sodium ions in the sodium carbonate solution.

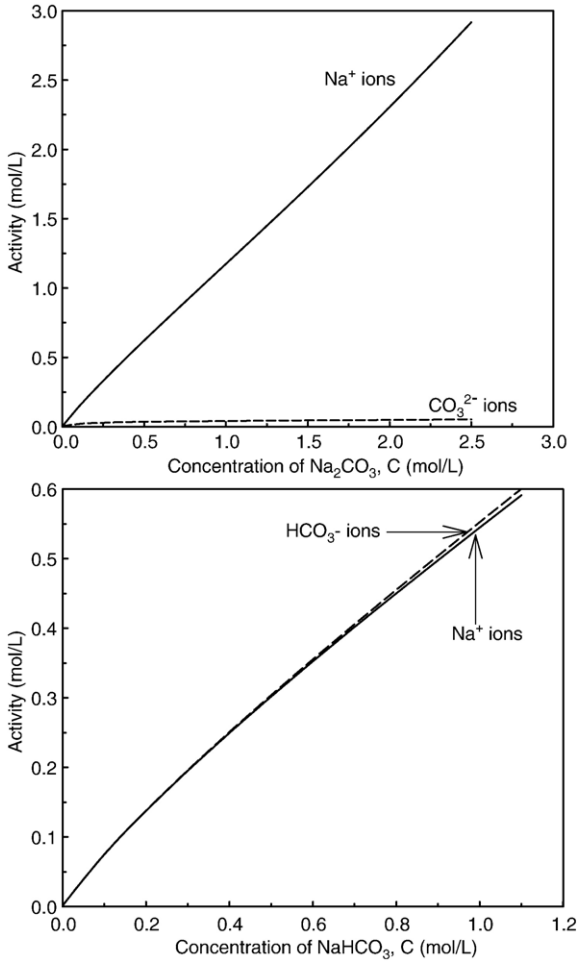

Fig. 5. Activities of ions versus salt concentration for Na_2CO_3 and $NaHCO_3$.

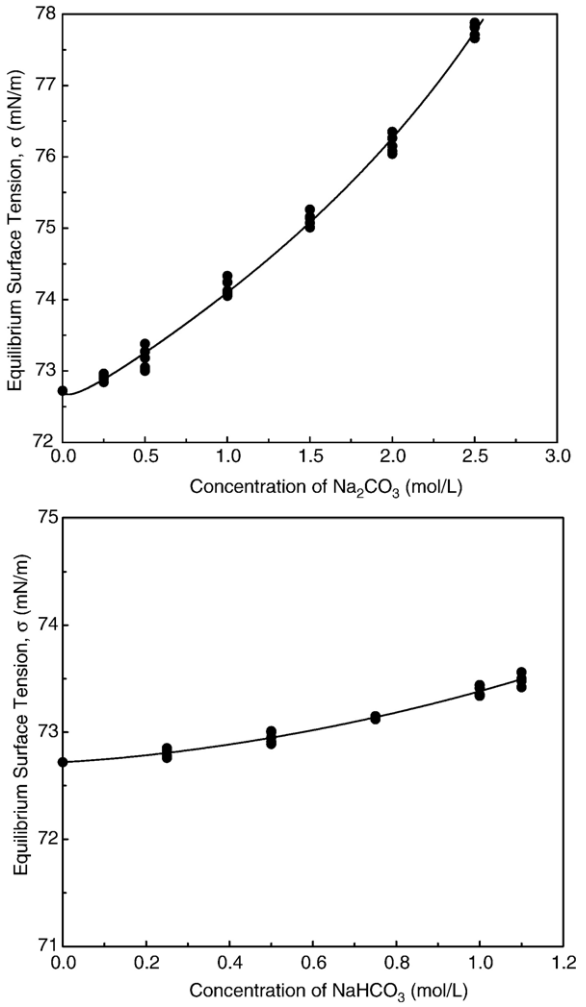

Fig. 6. Comparison between experimental data (points) and theoretical predictions (lines) described by Eq. (5) for the equilibrium surface tension of Na_2CO_3 and $NaHCO_3$ solutions versus concentration.

3.3. Comparison between experimental data and model prediction

The surface tension versus salt concentration can be calculated using Eq. (5) and compared with the experimental data for sodium carbonate and bicarbonate solutions. Comparison between the model prediction by theory, Eqs. (2)–(11), and the experimental data is shown in Fig. 6. The model parameters (K and Γ_∞) were obtained by the non-linear least-square regression analysis, which was carried out using the built-in function Solver in Microsoft Excel. The difference between a set of N experimental data points and the model for surface tension was minimized by the revised chi-square, χ^2, defined as $\chi^2 = \sum_{i=1}^{N} \left(\sigma_i^{\exp} - \sigma_i^{\text{theo}}\right)^2$. The minimization was obtained by adjusting the model parameters. The regression analysis assumed that the experimental uncertainties followed Gaussian statistics with equal standard deviation for all points. Then the standard deviation was determined as $(\chi^2/\nu)^{1/2}$, where ν is the degrees of freedom in the fit which is equal to the number of the experimental points less the number of parameters used in the minimization. The best fit with the model prediction has four free parameters (K_M, K_X, Γ_{M_∞} and Γ_{X_∞}). The obtained standard deviations were found to be 0.124 and 0.096 mN/m for the carbonate and bicarbonate solutions, respectively, which is significantly small, indicating that the prediction is statistically significant.

Results for the model parameters obtained from the regression analysis are shown in Table 4. Both the adsorption constant and maximum Gibbs surface excess for sodium ions are negative, showing that the adsorption of sodium ions from the carbonate and bicarbonate solutions is negative. For both the carbonate and bicarbonate ions, the adsorption constants and maximum Gibbs surface excess are positive, showing that these ions have a slight affinity for, and are adsorbed at the air–water interface similar to surfactants but at a much lower level.

3.4. Negative adsorption of carbonate and bicarbonate salts in relation to water structure

Now, knowing the adsorption constant and maximum Gibbs surface excess from the regression analysis, as shown in Table 4, the Gibbs surface excess (adsorption) for Na_2CO_3 and $NaHCO_3$ can be determined using Eqs. (6) and (7). The results are shown in Fig. 7. The Gibbs surface excess for sodium ions in carbonate and bicarbonate solutions is significantly negative and even more negative with increasing salt concentration. The Gibbs surface excess for carbonate ions is positive but its absolute magnitude is significantly smaller than the surface excess of sodium. The total adsorption shown in

Table 4
Equilibrium adsorption constant and maximum Gibbs surface excess obtained by the non-linear regression analysis of surface tension for $NaHCO_3$ and Na_2CO_3

Ions	Adsorption constant K (m^3/mol)	Maximum Gibbs surface excess Γ_∞ (mol/m^2)
Na^+ in Na_2CO_3 solutions	-1.698×10^{-4}	-1.678×10^{-6}
CO_3^{2-} in Na_2CO_3 solutions	8.162×10^{-4}	5.475×10^{-6}
Na^+ in $NaHCO_3$ solutions	-3.798×10^{-4}	-7.431×10^{-6}
HCO_3^- in $NaHCO_3$ solutions	1.393×10^{-4}	19.560×10^{-6}

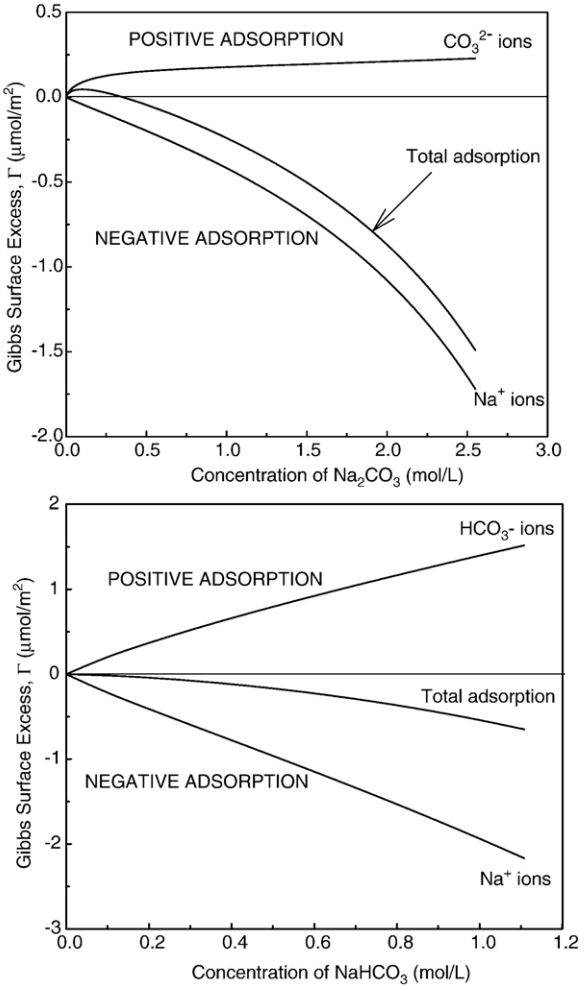

Fig. 7. Gibbs surface excess for adsorption of sodium, carbonate and bicarbonate ions from Na_2CO_3 and $NaHCO_3$ solutions as described by the Gibbs surface excess versus salt concentration by Eqs. (6) and (7).

Fig. 7 is equal to the sum of the Gibbs surface excesses of the cations and anions. For both salts, the Gibbs surface excess is negative and decreases with increasing salt concentration. The negative Gibbs surface excess strongly indicates that the sodium ions are excluded from the air–solution interface and prefer to associate with water molecules in the bulk solution.

The negative total Gibbs surface excess for sodium carbonate is higher than that for sodium bicarbonate. The difference in the negative Gibbs surface excess for the salts also indicates that sodium carbonate salt has a stronger affinity for water and is more difficult to float than sodium bicarbonate. This result fully agrees with the flotation results which show that strongly water structure making salts like sodium carbonate are difficult to float. The high floatability of sodium bicarbonate from its brine solution indicates that the salt does not make the water structure more ordered, allowing for collector adsorption and bubble attachment.

In addition to Na_2CO_3 and $NaHCO_3$, the surface tensions of other carbonates and bicarbonates such as K_2CO_3 and NH_4HCO_3 have also been measured. Again the effect of anions on salt adsorption and the surface tension was observed. Fig. 8 shows the surface tension results for these salts. It is evident that carbonate salts significantly increase the surface tension of water when compared to the results for bicarbonate salts.

The water structure making or breaking character of the salts has been confirmed by analyzing O–H (O–D) stretching vibrations using FTIR spectroscopy (Nickolov and Miller, 2005). Changes in the bandwidth and peak position of the O–H (O–D) stretching band reflect changes in H-bonding. The water structure making or breaking effects were studied in solutions of carbonates and bicarbonates in 4 wt.% D_2O in H_2O mixtures. The effect of salt concentration on the O–D stretching band is shown in Fig. 9. The FTIR spectroscopic results show a substantial water structure increase for Na_2CO_3 brines when compared to the FTIR spectroscopic features for $NaHCO_3$ brines. According to the O–D band analysis, Na_2CO_3 has a very strong water structure making effect, increasing the ice-like structure of water, while $NaHCO_3$ shows a weak water structure making effect. From these FTIR spectroscopic results and the negative Gibbs surface excess results it can be concluded that the water structure making and breaking effects of the anions

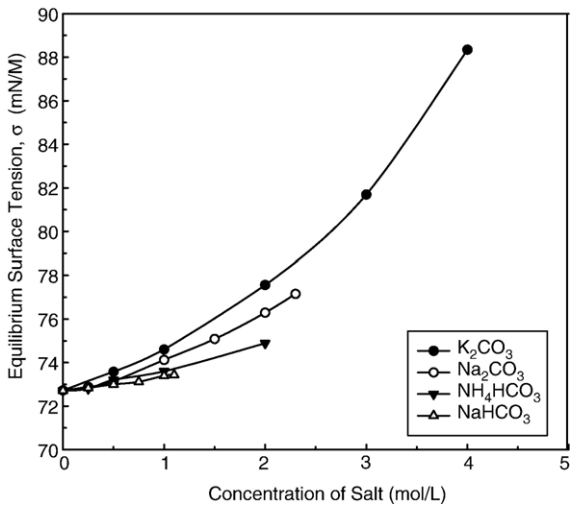

Fig. 8. Average equilibrium surface tension of brine solutions of carbonates and bicarbonates versus concentration up to saturation.

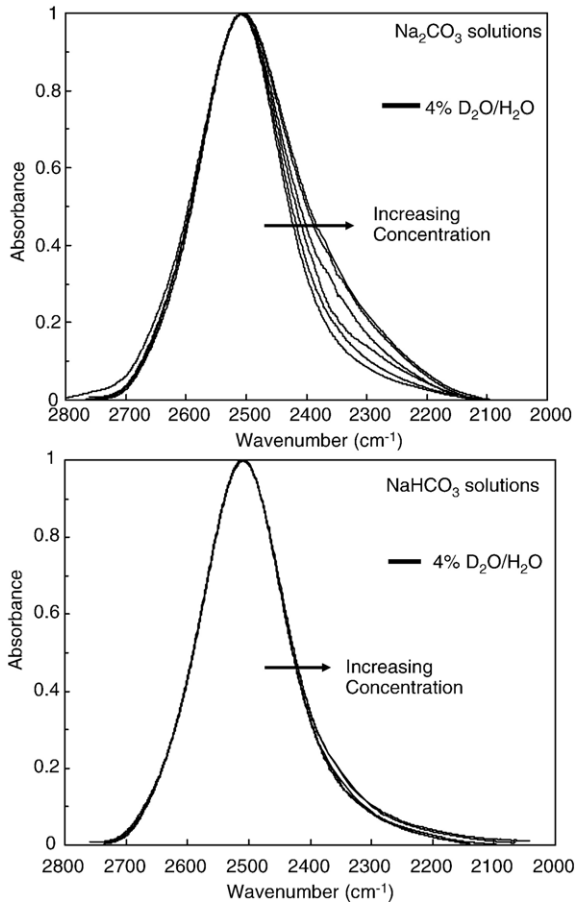

Fig. 9. O–D stretching bands in sodium carbonate and sodium bicarbonate aqueous solutions containing 4 wt.% D_2O as a function of salt concentration (a) Na_2CO_3 (2.0, 1.7, 1.25, 0.8, 0.4 M) and (b) $NaHCO_3$ (1.0, 0.7, 0.5, 0.4 M).

CO_3^{2-} and HCO_3^- play a significant role in the adsorption, surface tension and flotation of these salts.

4. Conclusions

In this paper, the adsorption of sodium, carbonate, and bicarbonate ions from their salt solutions at the air–brine has been investigated. The surface tension of the salts versus concentration was measured using pendant bubble tensiometry. The surface tension of the carbonate salts significantly increased as the concentration of Na_2CO_3 increased. On the other hand, the increase in the surface tension of $NaHCO_3$ solutions was not significant. The surface tension data are well compared with the Gibbs–Langmuir adsorption theory. The comparison shows that the negative adsorption of sodium from sodium carbonate solutions is significant, leading to the significant increase in surface tension of the brine solution of sodium carbonate. For sodium bicarbonate, both the negative adsorption of sodium and positive adsorption bicarbonate are strong and comparable, leading to small increase in the total adsorption (absolute value) and surface tension when compared to the results for sodium carbonate. The negative adsorption is correlated with the water structure making/breaking character of carbonate and bicarbonate. In particular, sodium carbonate is more strongly water structure making than bicarbonate and, therefore, is significantly excluded from the air–water interface. The strong structure making character of sodium carbonate may account for the fact that the direct flotation of trona from its brine is quite difficult. However, further studies are needed to explain why flotation of sodium bicarbonate salt is possible despite its weak structure making behavior.

Acknowledgements

The authors gratefully acknowledge the Australian Research Council. In addition, this collaborative research was supported by NSF under Grant No. INT-0207583.

References

Adamson, A.W, Gast, A.P., 1997. Physical Chemistry of Surfaces. John Wiley & Sons, Inc., New York. 784 pp.

Du, H., Rasaiah, J.C., Miller, J.D., submitted for publication. Structural and dynamic properties of concentrated alkali halide solutions: a molecular dynamics simulation study. Journal of Physical Chemistry B.

Garrett, D.E., 1991. Natural Soda Ash: Occurrences, Processing, and Use. Van Nostrand Reinhold, New York.

Hancer, M., Miller, J.D., 1999. The significance of interfacial water structure in the dodecyl amine flotation of potassium soluble salt minerals. SME Annual Meeting, Denver, Colorado, pp. 99–103. March, Preprint.

Hancer, M., Hu, Y., Fuerstenau, M.C., Miller, J.D., 1997. Amine flotation of soluble sulfate salts. Proceedings of the XX IMPC-Aachen, vol. 3, pp. 715–723. 21–26 September.

Hancer, M., Celik, M., Miller, J.D., 2001. The significance of interfacial water structure in soluble salt flotation systems. Journal of Colloid and Interface Science 235, 150–161.

Hartland, S., Hartley, R.W., 1976. Axisymmetric Fluid-Liquid Interfaces: Tables Giving the Shape of Sessile and Pendant Drops and External Menisci, with Examples of Their Use. Elsevier, Amsterdam. 782 pp.

Kim, H.T., Frederick Jr., W.J., 1988. Evaluation of Pitzer ion interaction parameters of aqueous electrolytes at 25 °C. 1. Single salt parameters. Journal of Chemical and Engineering Data 33 (2), 177–184.

Koneshan, S., Rasaiah, J.C., Lynden-Bell, R.M., Lee, S.H., 1998. Solvent structure, dynamics, and ion mobility in aqueous solutions at 25 °C. Journal of Physical Chemistry. B 102, 4193–4204.

Leja, J., 1982. Surface Chemistry of Froth Flotation. Plenum Press, New York. 758 pp.

Nickolov, Z., Ozcan, O., Miller, J.D., 2003. FTIR analysis of water structure and its significance in the flotation of sodium carbonate

and sodium bicarbonate salts. Colloids and Surfaces. A, Physicochemical and Engineering Aspects 224, 231–239.

Nickolov, Z.S., Miller, J.D., 2005. Water structure in aqueous solutions of alkali halide salts: FTIR spectroscopy of the OD stretching band. Journal of Colloid and Interface Science 287, 572–580.

Ozcan, O., Miller, J.D., 2002. Flotation of sodium carbonate and sodium bicarbonate salts from their saturated brines. Minerals Engineering 15 (8), 577–584.

Pitzer, K.S., 1973. Thermodynamics of electrolytes. I. Theoretical basis and general equations. Journal of Physical Chemistry 77 (2), 268–277.

Pitzer, K.S., Mayorga, G., 1973. Thermodynamics of electrolytes. II. Activity and osmotic coefficients for strong electrolytes with one or both ions univalent. Journal of Physical Chemistry 77 (19), 2300–2308.

Pitzer, K.S., Mayorga, G., 1974. Thermodynamics of electrolytes. III. Activity and osmotic coefficients for 2–2 electrolytes. Journal of Physical Chemistry 3 (7), 539–546.

Pitzer, K.S., Kim, J.J., 1974. Thermodynamics of electrolytes. IV. Activity and osmotic coefficients for mixed electrolytes. Journal of the American Chemical Society 96 (18), 5701–5707.

Wang, X., Li, M., Miller, J.D., 2002. Flotation as a process alternative for the treatment of trona resources. SME Annual Meeting, Phoenix, Arizona. February.

Weissenborn, P.K., Pugh, R.J., 1996. Surface tension of aqueous solutions of electrolytes: relationship with ion hydration, oxygen solubility, and bubble coalescence. Journal of Colloid and Interface Science 184, 550–563.